Limnol. Oceanogr., 58(4), 2013, 1207–1214
© 2013, by the Association for the Sciences of Limnology and Oceanography, Inc.
doi:10.4319/lo.2013.58.4.1207

Diel and lunar cycles of vertical migration extending to below 1000 m in the ocean and the vertical connectivity of depth-tiered populations

José Ochoa,* H. Maske, J. Sheinbaum, and J. Candela

Centro de Investigación Científica y de Educación Superior de Ensenada, Baja California, Ensenada, Baja California, México

Abstract

We measured diel migration with 11 acoustic Doppler current meter profilers and consistently found diel and lunar cycles of vertical migration from 250 m down to the bathypelagic (> 1000 m). These measurements come from year-long deployments in eight locations within the Gulf of Mexico. Diel vertical migration could be characterized, in depth and time, by a pulse of maximum vertical migration activity (PMV), which has a nearly fix phase relation to sunrise and sunset modulated by the lunar cycle. The vertical velocity of migrating biota is in the same direction as the PMV propagation, but it is significantly slower. This difference in velocity implies that the PMV cannot represent the migration pattern of one single population. The lunar cycle is evident down to 1000 m, where the upward migration delays in phase with the full moon. The extension of the diel and lunar cycles over 1000 m depth together with the difference in vertical migration velocity indicate that the surface irradiance signal is transmitted to bathypelagic depth by synchronized depth-tiered populations. A model in which particulate organics are recycled at different depths, similar to a bucket brigade, is consistent with these observations. This daily vertical connectivity is expected to affect the vertical transport of carbon down to the bathypelagic.

Zooplankton is a crucial agent in pelagic ecology, linking primary production with higher trophic levels. Zooplankton diel vertical migration is a global phenomenon linking the strata in the ocean transferring organic material toward greater depth (Angel 1989; Buesseler and Boyd 2009). The diel excursion of the 'sound scattering layer,' from ~ 150 m down to ~ 400 m, is easily observed with echo sounders and serves as a textbook example of negative phototaxis. This migration is commonly explained by a better food supply closer to the surface and predator avoidance by migration to deeper levels during the day, where visual detection is more difficult, a hypothesis calling for strict light control of vertical migration (Cohen and Forward 2009; Ringelberg 2010). The ample literature on diel vertical migration covers aspects of physiological control of the timing, energetic balances, and the effect on vertical transport of organics forming part of the biological carbon pump. Vinogradov (1962) proposed that zooplankton play a role in the vertical transport of organic material within the mesopelagic depth range (bottom of the euphotic zone to 1000 m), suggesting the term 'ladder of migrations' for the diel migration of different populations of zooplankton covering different depth ranges. The literature agrees that light triggers the migration; solar eclipses perturb the cycle, and even lunar eclipses have significant effects (Tarling et al. 1999), but the specific property of irradiance that is acting on the organisms is not clear (Cohen and Forward 2009; Ringelberg 2010).

The present study is based on data from 11 Acoustic Doppler Current Profilers (ADCPs) deployed in the western Gulf of Mexico. ADCPs infer ocean currents, measuring the changing distance of sound-scattering disturbances relative to the origin of sound. ADCP data have been employed in migration studies from their inception (Plueddemann and Pinkel 1989). With regard to zooplankton, ADCPs provide two types of information: the change in the distance of the sound-scattering disturbances converted into the along-beam velocity component and the echo strength. The first signal measures a mean velocity of the scatterer's cloud; it is a bulk measurement in which different fractions might even go in opposite directions. This is a real possibility with zooplankton, as reverse migrations are not uncommon. The echo strength depends on the size, amount, and magnitude of the sound disturbances that cause the backscattering. The scattering might be related to the concentration of organisms, their orientation relative to the sound source, and even the turbulence produced by the swimming organisms. The time coverage and vertical resolution, approximately 10 m for the 75 kHz ADCPs used here, are nowadays impossible to match with net sampling or optical profilers. The latest has higher vertical resolution but limited sample size and deployment duration. Nets can provide detailed taxonomic composition and could match a 10 m vertical resolution, but only over a limited depth range and short periods of time. Multi-frequency echo sounders have been used to document depth and size distributions (Lawson et al. 2008). Time course observations of echo sounders yield information on migration patterns, with time derivatives allowing estimates of migration velocities. To study the general migration behavior, within the mesopelagic zone, ADCP data are amply used because they provide information with sufficient resolution and coverage in terms of both depth and time. With ADCP data alone, as in this study, the lack of organism identification is a substantial limitation; thus, we have emphasized this deficiency by referring to 'scatterers population.' Here, we combined data from 11 ADPCs to document the migration patterns over yearly periods at different depths. This large database, which

* Corresponding author: jochoa@cicese.mx

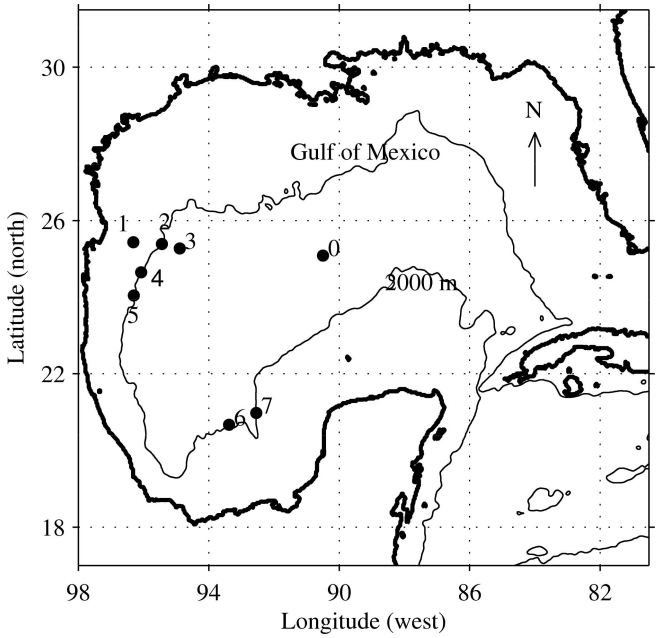

Fig. 1. Map of the Gulf of Mexico showing mooring locations and the 2000 m isobath.

includes several bathypelagic measurements, allowed the observation of mean patterns previously not recognized.

Methods

The vertical velocity of migrating biota in the mesopelagic zone was measured with nine upward-looking and two downward-looking 75 kHz ADCPs (RDI) at eight locations within the Gulf of Mexico (Fig. 1; Table 1). At each of the moorings, named WG-0 to WG-7, one or two ADCPs provided data for this study. Five of the 11 ADCPs measured levels shallower than 550 m, two measured levels in the range of ~ 700 to ~ 400 m, and four measured levels from ~ 1200 to ~ 800 m (Table 1). At three of the moorings, two ranges were measured simultaneously. All ADCPs worked properly, and full records were recovered.

ADCP data analysis—All upward-looking instruments were configured for 10 m thick bins with 18 individual measurements evenly distributed in time and averaged to produce one record every 30 min. The two downward-looking ADCPs were configured for 16 m thick bins with 12 individual measurements evenly distributed for one recording every 30 min. The Doppler principle allows an estimate of the velocity component along the beam with a depth resolution, for the 75 kHz ADCPs, of typically 10 m and a maximum range of approximately 500 m, depending on the echo strength. Heading, pitch, and roll of the instrument as well as depth via a pressure sensor are measured for proper velocity estimates. Because the measurement from a single measurement, or ping, is quite noisy, the average of as many as possible individual measurements, or pings, is recommended. Ott (2005) has analyzed the uncertainties in velocities given the ADCP's attitude errors. The common angle from the vertical is 20°; therefore, the error of the vertical component is smaller than that of the horizontal. Using the manufacturer specifications, the error for a single ping measurement in a 10 m bin has a standard deviation of 0.118 m s^{-1} in any of the horizontal velocity components. With 18 measurements, or pings, the error reduces to 0.028 m s^{-1} (i.e., $0.118/\sqrt{18}$ m s^{-1}). Under ideal conditions (i.e., homogeneity in the flow field and vertically aligned instrument), the vertical velocity error is smaller than that by the factor cos(80°) = 0.1736 (Ott 2005, Eq. 2). This leads to a standard error of 0.0048 m s^{-1} in vertical velocity for the 18 pings average in a 10 m bin. Given the lack of homogeneity in the flow field, the instrument attitude errors, and even the manufacturer processing, the actual error is larger (Ott 2005). The scattering features that are most responsible for the echo strength are perturbations, in the sound speed, with a size of one wavelength of the acoustic waves. Since the sound speed is ~ 1500 m s^{-1}, 75 kHz ADCPs are measuring the motion of scattering features, including organisms, with size of about 2 cm. ADCPs have been used to map zooplankton distributions in many studies, and when combined with net haul samplings they offer estimates of standing stock biomass (Biggs and Ressler 2001; Ressler 2002).

The instrument's vertical velocity is estimated via the pressure gauge; therefore, the vertical motion of the scattering biota relative to the sea surface is easily derived. The instrument's depth accuracy, reported by the manufacturer, is ± 5 m. At WG-0 the ADCP moored at ~ 368 m reached a maximum depth of 450 m and a minimum of

Table 1. Positions, depths, and recording duration of 11 LR75-kHz ADCPs at eight moorings. The mean sitting depths of ADCPs and orientation ('d' for looking downward and 'u' upward) are shown in the last column.

Mooring name	Latitude (°N)	Longitude (°W)	Bottom depth (m)	Date		Mean depth (m)
				Start	End	
WG-0	25.086	90.500	3640	11 May 2003	27 Aug 2004	368u 1233u
WG-1	25.436	96.314	447	22 Dec 2004	09 Nov 2005	436u
WG-2	25.389	95.439	2000	26 Aug 2004	11 Nov 2005	529u 1240u
WG-3	25.272	94.890	3524	26 Aug 2004	11 Nov 2005	1268u
WG-4	24.651	96.078	1996	26 Aug 2004	11 Nov 2005	501u
WG-5	24.045	96.301	2003	26 Aug 2004	11 Nov 2005	554u 1263u
WG-6	20.668	93.382	2149	25 Jul 2009	04 Aug 2010	256d
WG-7	20.978	92.524	2164	06 Aug 2010	04 Sep 2011	272d

19395590, 2013, 4, Downloaded from https://aslopubs.onlinelibrary.wiley.com/doi/10.4319/lo.2013.58.4.1207 by Moss Landing Marine Labs, Wiley Online Library on [06/11/2026]. See the Terms and Conditions (https://onlinelibrary.wiley.com/terms-and-conditions) on Wiley Online Library for rules of use; OA articles are governed by the applicable Creative Commons License

361 m, and, hence, it had a maximum excursion of 89 m; the other ADCPs had maximum excursions of less than 10 m. Linear interpolations were used to produce profiles at fixed depths with a 10 m interval. To obtain the scatterer's velocity, the instrument's velocity must be subtracted from the Doppler measurement. Hence, the noise in migration velocities depends also on the stability and precision, rather than the accuracy, of the depth recordings. The instrument's depth estimate is deduced via a pressure sensor and its vertical velocity via finite differences of successive recordings. The uncertainty in the instrument's vertical velocity can be found from idle measurements while the ADCPs are recording on deck before deployment. These periods lasted, considering the nine ADCPs, from 19 to 70 h and provided a total of 670 velocity estimates, which are noise. The maximum of such errors is 0.0006 m s^{-1}, and the root mean square is 0.00015 m s^{-1}.

Adjusting data to sunrise and sunset—The migration timing of the scattering populations maintained a nearly fixed phase relation to dusk and dawn. Here, a mean cycle follows from averaging a set of individual cycles timed relative to sunrise and sunset. Figure 2B shows the modulation along the year of a set of individual cycles, in this example, of the vertical velocity of a 150 m thick layer; from 350 to 500 m depth. A linear interpolation with a 3 min interval, covering from 5 h before to 5 h after sunrise, was done for each diel cycle available in the time series. A similar interpolation covers the sunset for vertical velocity and echo strength. This resampling allows a proper averaging of 'aligned' cycles, as clearly shown in Fig. 2A. Mean diel cycles are averages of all available cycles at each depth level. The period between sunrise and sunset at the geographic location varied between 10.6 and 13.7 h through the year (http://www.srrb.noaa.gov/highlights/sunrise/sunrise.html); in response, the scattering populations adjust the time of occupancy in the upper or lower depth strata, keeping the migration timing with respect to a combination of sunrise, sunset, and lunar cycle.

Results

The ADCPs registered diel cycles of scatterers throughout the year demonstrating migration pulses that were timed to the sunrise and sunset; to arrive at the mean pulse pattern the timing was set by the location-specific astronomical sun cycle (Fig. 2). The pulses, one near to sunrise and the other to sunset, are characterized by the maximum speed and the time of their occurrence as a function of depth. As shown in Fig. 3, both pulses of maximum vertical migration activity (PMV) occur monotonically with depth. The PMV timing, relative to sunrise and sunset and labeled here as 06:00 and 18:00 h, shows its vertical propagation in Fig. 3A (vertical velocity). A second-degree polynomial fit of the PMV depth vs. time measurements gives

$$\text{downward migration, } Z_{\text{PMV,d}}\ [\text{m}] = -3175.2 + 823.4\ \text{t} - 37.276\ \text{t}^2 \quad (R^2 = 0.99) \tag{1}$$

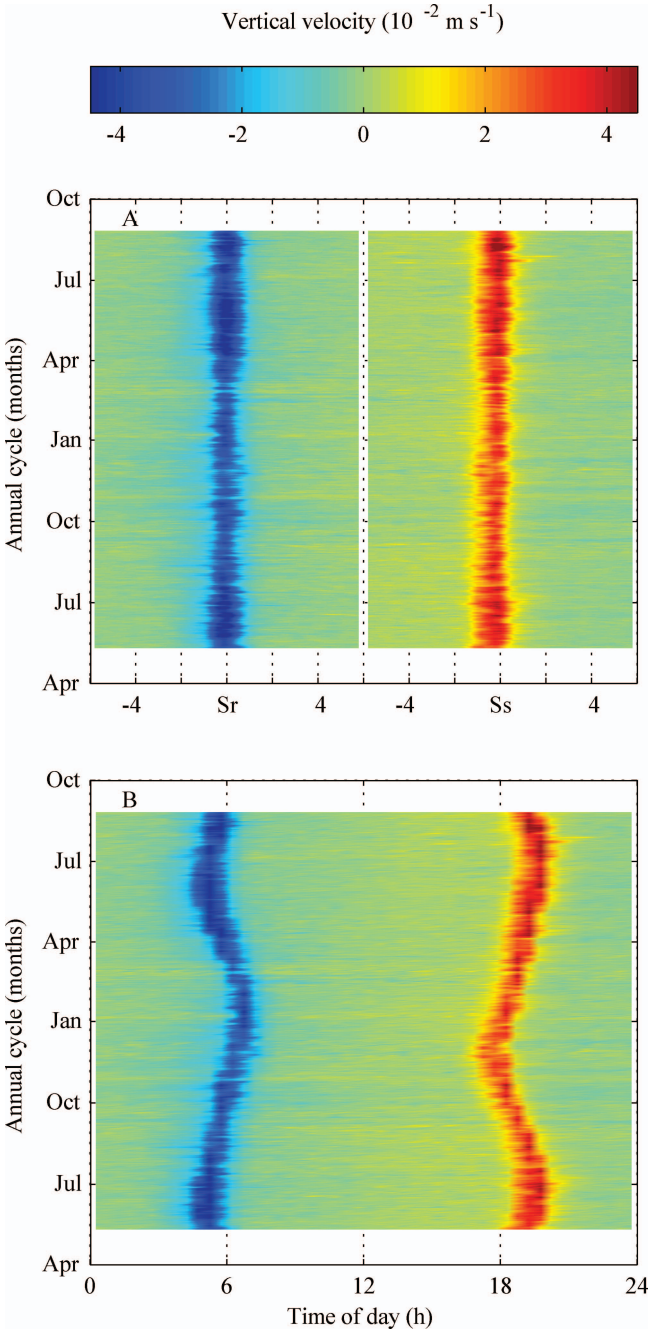

Fig. 2. Color-coded diagram, with the scale at the top in cm s^{-1}, of the vertical velocity in the layer from 350 to 500 m below the surface, as a function of time during the day and date throughout the WG-0 measuring period (Table 1). For frame A the abscissa axes are hours relative to sunrise (Sr) and sunset (Ss), and for frame B they are the local time in hours.

$$\text{upward migration, } Z_{\text{PMV,u}}\ [\text{m}] = +630.68 + 450.38\ \text{t} - 25.642\ \text{t}^2 \quad (R^2 = 0.99) \tag{2}$$

where time (t) is in hours, so that sunrise is at 06:00 h and sunset at 18:00 h. These polynomials are shown by the continuous black lines in Fig. 3A. In Fig. 3B (ΔEcho) the diel echo strength pattern varies with depth, with minimum/

19395590, 2013, 4, Downloaded from https://aslopubs.onlinelibrary.wiley.com/doi/10.4319/lo.2013.58.4.1207 by Moss Landing Marine Labs, Wiley Online Library on [06/11/2026]. See the Terms and Conditions (https://onlinelibrary.wiley.com/terms-and-conditions) on Wiley Online Library for rules of use; OA articles are governed by the applicable Creative Commons License

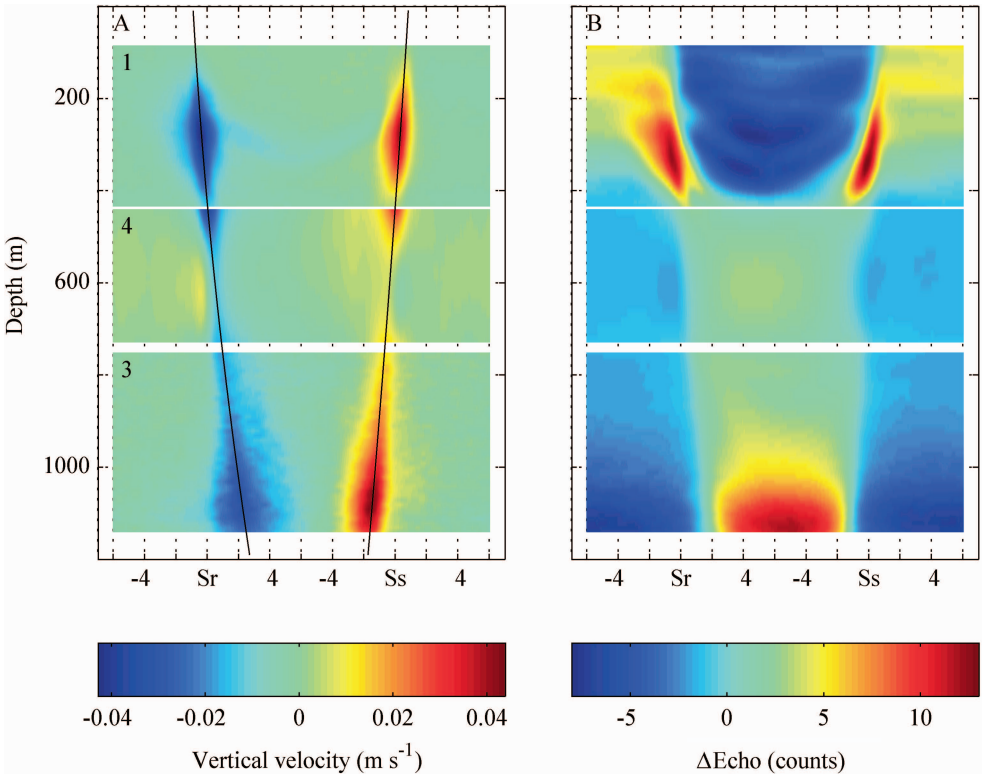

Fig. 3. Mean cycles of vertical velocity (A) and echo anomaly (B) in the abscissa time within a cycle, in hours, relative to sunrise (Sr) and sunset (Ss), in the ordinate depth in meters. At each depth level, the composite average of year-long records produces the mean diel cycle. The velocity color scale (in m s^{-1}) applies to the section labeled 1; in section 4 the velocity is multiplied by 4, and in section 3 it is multiplied by 3. In frame B ΔEcho shows the echo strength anomaly, in RDI relative counts; at each depth level its mean value is subtracted.

maximum relative echo during daytime above/below 400 m. No corrections have been applied to the echo, but variations at a given level are comparable (van Haren 2007).

Figure 4 shows the propagation velocity of the PMV, calculated by differentiation of Eqs. 1 and 2. Two relative maxima were found in the PMV's maximum speed, one at 220 m depth with speeds of ~ 0.04 m s^{-1} and the other at 1100 m with speeds of ~ 0.015 m s^{-1}; at other depths the typical migration speeds were ~ 0.01 m s^{-1} (Fig. 4). These speeds (i.e., the maxima speed during the mean cycle) are significantly lower than the propagation velocities of the PMV. For this reason, we considered the possibility that the reduced vertical velocity of the migrating scattering biota was due to the averaging of the echoes of migrating scatterers and suspended, non-migrating scatterers. When we compared the daily echo strength amplitude with vertical velocity at 425 and 1075 m depth we found correlations that passed through the origin, indicating that the echo originated from vertically moving particles.

The mean vertical excursion per day follows from integration of the mean vertical velocity. These excursions are ~ 75 m at 250 m and ~ 50 m at 1100 m. They do not differ that much because the low speed migration at 1100 m is compensated for by longer swimming duration.

The lunar cycle—These data show that for lunar cycles, for example, at 250 and 1100 m, the echo strength increases

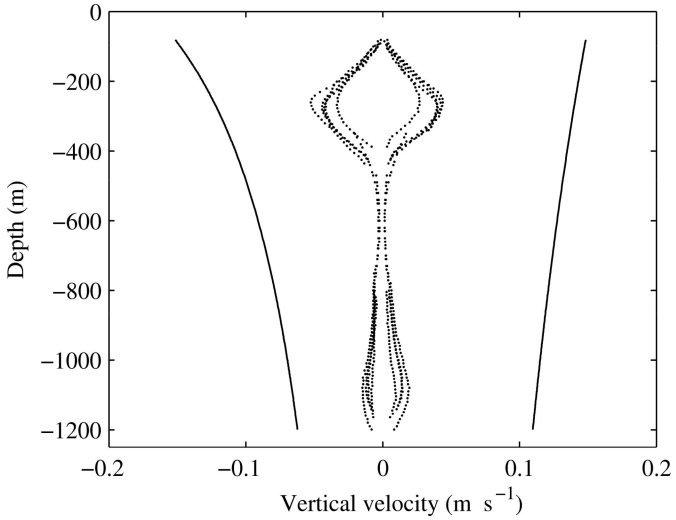

Fig. 4. In dots, the maximum upward (positive) and downward (negative) biota migration velocities from independent mean diel cycles. The PMV vertical propagation velocity, computed by differentiation of Eqs. 1 and 2, is shown in the solid line.

19395590, 2013, 4, Downloaded from https://aslopubs.onlinelibrary.wiley.com/doi/10.4319/lo.2013.58.4.1207 by Moss Landing Marine Labs, Wiley Online Library on [06/11/2026]. See the Terms and Conditions (https://onlinelibrary.wiley.com/terms-and-conditions) on Wiley Online Library for rules of use; OA articles are governed by the applicable Creative Commons License

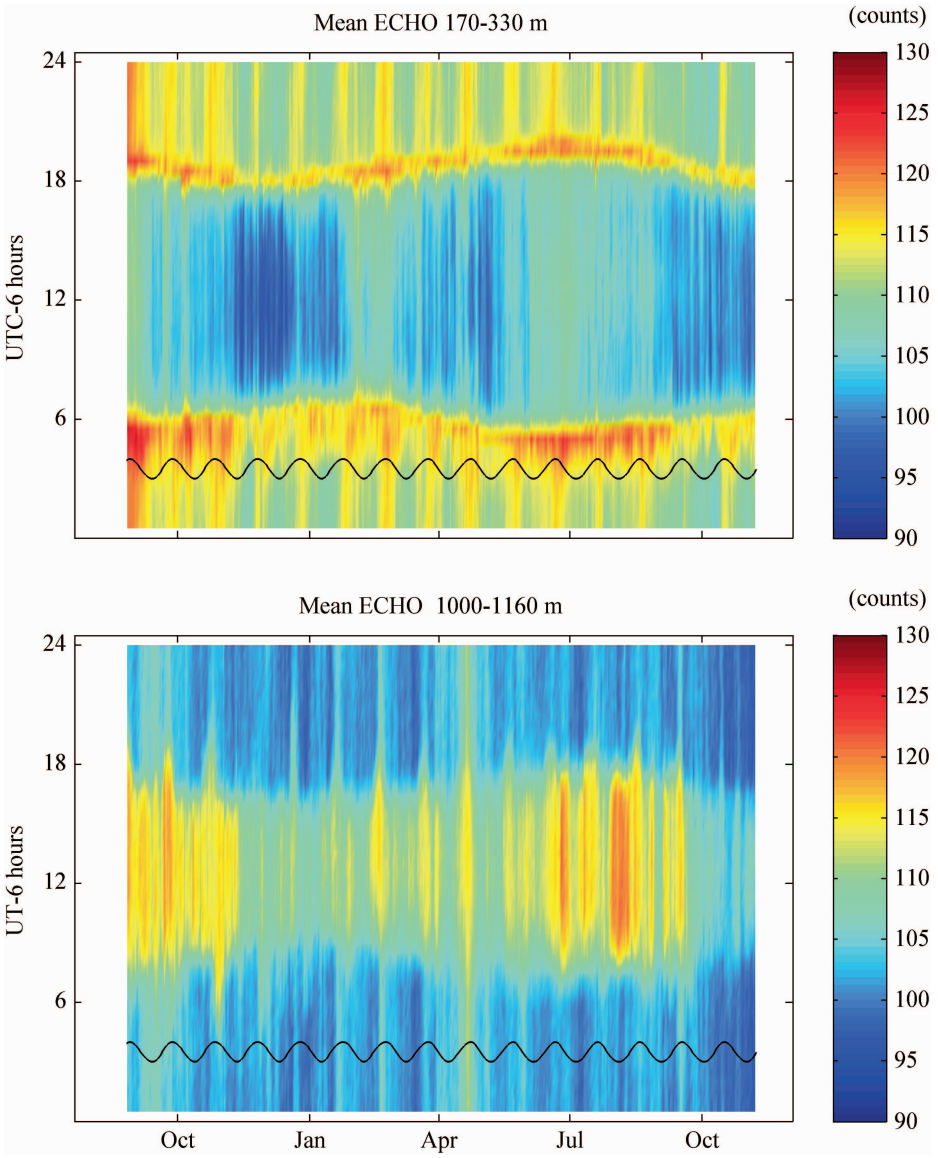

Fig. 5. Color-coded distribution of echo strength, in RDI relative counts, as a function of time during each diel cycle, in local time (Universal Time Coordinated [UTC]–6 h), and date through the measuring period. Superimposed, at about 05:00 h, is the lunar cycle with increasing intensity upwards. Simultaneous data from three ADCPs were averaged (A) over the 170–330 m depth interval and (B) over the 1000–1160 m depth range.

during the full moon nights and decreases during the new moon (Fig. 5). The data also show that even below 1000 m the upward migration is delayed, relative to sunset, during the full moon (Fig. 6).

Discussion

Plueddemann and Pinkel (1989) show (in their fig. 5) the average of 15 daily cycles from a 38 kHz ADCP in the eastern North Pacific, and their mean cycle pattern is remarkably similar to the findings of van Haren (2007, their fig. 3), which also show a similar pattern for the depth range of 800–1300 m off the Canary Islands. The similarity in migration pattern in other oceans indicates that the migration pattern is not location specific. The velocities that Fig. 4 shows (i.e., maximum vertical velocities of mean diel cycles) compare well with measured values between 0.01 and 0.05 m s^{-1} reported by van Haren (2007), Roe et al. (1996), and Wiebe et al. (1992). These migration velocities are significantly lower than the propagation velocity of the PMV, which is from −0.05 to −0.16 m s^{-1} for the downward and 0.1 to 0.15 m s^{-1} for the upward migration (Fig. 4).

These data support the existence of different depth-tiered scattering populations, because the migration velocity of the scattering biota is not constant (Fig. 2) and the diel echo strength pattern varies with depth (Fig. 3; ΔEcho). The mean vertical excursions and the difference between the PMV and migration velocities are incompatible with one population migrating over more than 1000 m but could

19395590, 2013, 4, Downloaded from https://aslopubs.onlinelibrary.wiley.com/doi/10.4319/lo.2013.58.4.1207 by Moss Landing Marine Labs, Wiley Online Library on [06/11/2026]. See the Terms and Conditions (https://onlinelibrary.wiley.com/terms-and-conditions) on Wiley Online Library for rules of use; OA articles are governed by the applicable Creative Commons License

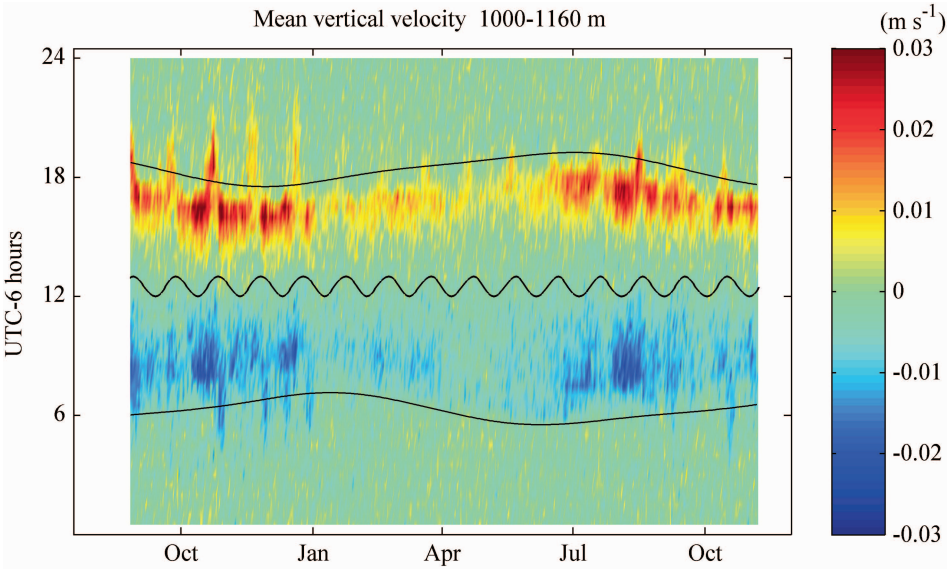

Fig. 6. Average migration velocity of particles between 1000 and 1160 m (in m s^{-1}), similar to and from the corresponding data set of Fig. 5B. Superimposed at 12:00–13:00 h is the lunar cycle, with increasing intensity upwards. The timing of upward migration is delayed in phase with increasing moonlight. The timing of the sunrise and sunset is indicated in solid traces.

be explained if several populations at different depths migrate, sequentially, in a coordinated fashion, similar to a relay race, but with the next population starting their migration before the previous population arrives.

The low amplitude excursions (i.e., order of ~ 100 m) imply that the scattering population at 1000 m depth is exposed to such low daylight irradiance that it would be masked by the irradiance produced by internal light sources.

In situ irradiance below the euphotic zone—Little information has been published about the diffuse attenuation coefficient (k_d) in the mesopelagic and bathypelagic ocean because it is difficult to separate the solar irradiance from internal light sources (i.e., bioluminescence and Cerenkov emission from either ^{40}K beta decay or Muons produced by Neutrino). At such depths, the contribution of internally produced irradiance has spectra with significant overlap with the residual daylight (Mobley 1994; Reynold and Lutz 2001) and comprises a significant portion of in situ irradiance (Denton 1990 Amram et al. 2000). At depths below 500 m, the wavelength dependence of light attenuation in the ocean leads to a narrow band irradiance centered on 480 nm (we follow the convention of using wavelengths in the vacuum). The k_d for 440 to 500 nm within mesopelagic waters can be assumed to be between 0.017 and 0.027 m^{-1}, similar to that of the clearest ocean water (Smith and Baker 1981). Young et al. (1980) measured, for ~ 480 nm wavelengths, a $k_d \approx 0.035$ m^{-1} at depths between 205 and 380 m. One approach to estimate the changes in k_d assumes a constant ratio of absorption to scattering coefficient (Kirk 1991). Measurements show a continuous decline in attenuation up to depths of about 2000 m (Riccobenne et al. 2007), indicating that k_d in the mesopelagic is not constant. Given inputs of (1) clear sky, (2) wind of 5 m s^{-1}, (3) chlorophyll: (<100 m) = 0.1 mg m^{-3} (> 100 m) = 0, and (4) clear water attenuation (Smith and Baker 1981), the Hydrolight version 4.3 model yields an average diffuse attenuation of 0.025 m^{-1} for the irradiance band between 430 and 480 nm. This implies a summer solstice noon solar irradiance of 10^{-8} μmol m^{-2} s^{-1} at 1000 m depth in the Gulf of Mexico. The estimate of internal irradiance from ^{40}K beta decay is 200 photons cm^{-2} s^{-1} (Learned and Mannheim 2000); hence, the depth of equal solar irradiance would be at most 1300 m, but, given other internal light sources, it must be shallower. In Hawaii's proximity, the bioluminescence irradiance was found to balance daylight solar irradiance at 700 m, near a peak concentration of bioluminescent animals (Young 1983). Hence, the synchronization of diel cycles below 1000 m is unlikely to be controlled by solar irradiance (Denton 1990).

The lunar cycle—Oceanic zooplankton have been shown to respond to the lunar cycle. A lunar cycle of zooplankton biomass in the top 90 m was observed in the subtropical Atlantic by Hernández-León et al. (2010), and a lunar cycle in the ADCP echo strength was detected between 900 and 1300 m by van Haren (2007). Our data show lunar cycles in echo strength (Fig. 5) and the migration timing (Fig. 6). At the sea surface, the irradiance of the moon is approximately 5×10^{-5} that of noon solar irradiance (Miller and Turner 2009); therefore, at 1000 m depth and assuming k_d = 0.025 m^{-1} (*see* above), the lunar irradiance would be ~ 10^{-15} of midday solar irradiance at the surface. Furthermore, the upward migration at this depth initiates before sunset (Fig. 3), when the lunar irradiance is insignificant compared to solar irradiance.

The bucket brigade model—One possible interpretation for the pulse of maximum vertical migration activity

19395590, 2013, 4, Downloaded from https://aslopubs.onlinelibrary.wiley.com/doi/10.4319/lo.2013.58.4.1207 by Moss Landing Marine Labs, Wiley Online Library on [06/11/2026]. See the Terms and Conditions (https://onlinelibrary.wiley.com/terms-and-conditions) on Wiley Online Library for rules of use; OA articles are governed by the applicable Creative Commons License

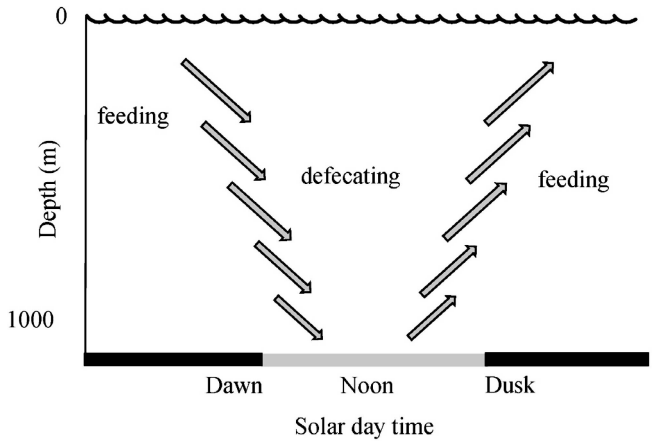

Fig. 7. The bucket brigade model of sequential migration.

(PMV) depth-time pattern (Fig. 3) is a synchronized sequence of migrations, in which the proximate population starts its migration before the prior population reaches such depth, with the vertical propagation of the PMV faster than the actual migration speeds. These sequentially migrating populations behave like a bucket brigade (BB), in which each population transports organics consumed at their shallower nighttime strata to their deeper daytime strata, where defecation supplies the organics to the population below (Fig. 7). This model is consistent with (1) the high propagation velocity of the PMV, (2) the reason for which there is a gain for populations in the mesopelagic ocean from exhibiting diel migration of relatively small vertical amplitude, and (3) the reason for which the daily timing of these migrations with greater depth is successively later in the morning and earlier in the afternoon, thus maximizing the period of feeding in the upper stratus but still minimizing the contact with the above population. The BB model indicates that the populations that are too deep to synchronize their migrations through the daylight and moonlight cycle take their timing signal for migration from the migration activity of the shallower populations up to the surface population. This signal control does not work for the up-migration, when the shallower population migrates later. The up-migration timing is set by a still-unknown signal. The BB model indicates connectivity, from surface to ~ 1000 m depth, which maintains the diel migration cycle with a specific phase vs. depth relation, even with the lunar cycle fluctuations.

The upper depth level of a population should be close to the lower depth level of the population residing above it, and, therefore, defecation during daylight can effectively augment the food concentration via coprophagy (Lampitt et al. 1990). The pattern indicates a BB by which repackaged particulate organics are handed, mainly, from one population to the one beneath it, in daily cycles. Data that are consistent with the BB model are the following: (1) the fast PMV propagation compared to the organisms' speeds, (2) the fact that migration and echo patterns differ with depth, indicating separate populations, and (3) the migration timing, which is strictly synchronized to near-surface light.

The BB model indicates a new concept of zooplankton ecology in the mesopelagial; it will be challenging to test it by net sampling and visual profiling. Visual observations might document living organisms and fecal pellets. The BB model, which differs from the hunger–satiation–migration hypothesis, might explain the apparent contradiction that species at depth contained phytoplankton pigments, although they were reported not to migrate (Enright 1977). The BB interpretation indicates a chain of depth-distributed zooplankton populations that gain food access away from their own fecal pellets by small vertical migrations, optimized in energy expenditure. Predator avoidance might play a role for some populations and be secondary or even irrelevant for others. A related, but different, model, named 'cascading migrations' (Bollens et al. 2011), proposes that the members of a linear hierarchical food chain, consisting of predator–prey pairs, show coordinated vertical migration. If the vertical migration happens to avoid visual predators, one implication is top predators closer to the surface. In the BB model, the vertical neighbors are not necessarily predator–prey pairs, and the vertical trophic structure is not necessarily hierarchical. The changes in fecal pellet characteristics observed by Wilson et al. (2008) indicate that latitudinal gradients in migration and BB populations exist.

The BB model and vertical transport of carbon—Transport of particulate organic material from the surface toward the bottom, the biological pump, is responsible for sequestering approximately 25% of the atmospheric fossil-fuel CO_2. It has been discussed that zooplankton diel migration facilitates the downward transport of organic material toward greater depth, in which case it forms part of the biological pump (Zhang and Dam 1997; Yamaguchi et al. 2002). In the BB model, recycled particulate organic material is ratcheted downward during the migration period (Fig. 7). When the fecal particles are recycled through coprophagy, some portion of the pellets should also be fractionated. This coprorhexy (Iversen and Poulsen 2007) should facilitate microbial degradation of organics (Steinberg et al. 2000). The overall effect on the vertical transport of organics might be a slowing of transport rate.

The BB model sets a framework but leaves questions unanswered: What are the mechanisms that communicate the timing of migration from one population to the next? Is the lunar cycle transmitted by the same mechanisms as the diel cycle to the lower populations?

Acknowledgments

Financing and data for the present work were obtained from the Outer Continental Shelf Study, Mineral Management Service 2006-001, Bureau of Ocean Energy Management, Regulation and Enforcement 2010-044, and Convenio de Servicios 428229851 (Medición y Análisis Metoceánico del Golfo de México, etapa 2009–2013. Pemex Exploración y Producción, Petróleos Mexicanos). We are grateful for the anonymous reviewers' criticism, corrections, and remarks; they were fundamental for the improvement of the study.

References

Amram, P., and others. 2000. Background light in potential sites for the ANTARES undersea neutrino telescope. Astropart. Phys. **13:** 127–136, doi:10.1016/S0927-6505(99)00118-8

19395590, 2013, 4, Downloaded from https://aslopubs.onlinelibrary.wiley.com/doi/10.4319/lo.2013.58.4.1207 by Moss Landing Marine Labs, Wiley Online Library on [06/11/2026]. See the Terms and Conditions (https://onlinelibrary.wiley.com/terms-and-conditions) on Wiley Online Library for rules of use; OA articles are governed by the applicable Creative Commons License

Angel, M. V. 1989. Does mesopelagic biology affect the vertical flux?, p. 155–173. *In* W. H. Berger, V. S. Smetacek, and G. Wefer [eds.], Productivity of the ocean: Present and past. Wiley.

Biggs, D. C., and P. H. Ressler. 2001. Distribution and abundance of phytoplankton, zooplankton, ichthyoplankton, and micronekton in the deepwater Gulf of Mexico. Gulf Mex. Sci. **19:** 7–29.

Bollens, S., G. Rollwagen-Bollens, J. A. Quenette, and A. B. Bochdansky. 2011. Cascading migrations and implications for vertical fluxes in pelagic ecosystems. J. Plankton Res. **33:** 349–355, doi:10.1093/plankt/fbq152

Buesseler, K. O., and P. W. Boyd. 2009. Shedding light on processes that control particle export and flux attenuation in the twilight zone of the open ocean. Limnol. Oceanogr. **54:** 1210–1232, doi:10.4319/lo.2009.54.4.1210

Cohen, J. H., and R. B. Forward. 2009. Zooplankton diel vertical migration: A review of proximate control. Oceanogr. Mar. Biol. Annu. Rev. **47:** 77–110, doi:10.1201/9781420094220.ch2

Denton, E. J. 1990. Light and vision at depth greater than 200 m, p. 127–148. *In* P. J. Herring, A. K. Campbell, M. Whitfield, and L. Maddock [eds.], Light and life in the sea. Cambridge Univ. Press.

Enright, J. T. 1977. Diurnal vertical migration: Adaptive significance and timing. Part 1. Selective advantage: A metabolic model. Limnol. Oceanogr. **22:** 856–872, doi:10.4319/lo.1977.22.5.0856

Hernández-León, S., G. Franchy, M. Moyan, I. Menéndez, C. Schmoker, and S. Putzeys. 2010. Carbon sequestration and zooplankton lunar cycles: Could we be missing a major component of the biological pump? Limnol. Oceanogr. **55:** 2503–2512, doi:10.4319/lo.2010.55.6.2503

Iversen, M. H., and L. K. Poulsen. 2007. Coprorhexy, coprophagy, and coprochaly in the copepods *Calanus helgolandicus*, *Pseudocalanus elongates*, and *Oithona similis*. Mar. Ecol. Prog. Ser. **350:** 79–89, doi:10.3354/meps07095

Kirk, J. T. O. 1991. Volume scattering function, average cosines, and the underwater light field. Limnol. Oceanogr. **36:** 455–467, doi:10.4319/lo.1991.36.3.0455

Lampitt, R. S., T. Noji, and B. von Bodungen. 1990. What happens to zooplankton faecal pellets? Implications for material flux. Mar. Biol. **104:** 15–23, doi:10.1007/BF01313152

Lawson, G. L., P. H. Wiebe, T. K. Stanton, and C. J. Ashjian. 2008. Euphausiid distribution along the Western Antarctic Peninsula—part A: Development of robust multi-frequency acoustic techniques to identify euphausiid aggregations and quantify euphausiid size, abundance, and biomass. Deep-Sea Res. II **55:** 412–431, doi:10.1016/j.dsr2.2007.11.010

Learned, J. G., and K. Mannheim. 2000. High-energy neutrino astrophysics. Annu. Rev. Nucl. Part. Sci. **50:** 679–749, doi:10.1146/annurev.nucl.50.1.679

Miller, S. D., and R. E. Turner. 2009. A dynamic lunar spectral irradiance data set for NPOESS/VIIRS day/night band nighttime environmental applications. IEEE Trans. Geosci. Remote Sens. **47:** 2316–2329, doi:10.1109/TGRS.2009.2012696

Mobley, C. D. 1994. Light and water. Radiative transfer in natural waters. Academic Press.

Ott, M. W. 2005. The accuracy of acoustic vertical velocity measurements: Instrument biases and the effect of zooplankton migration. Cont. Shelf Res. **25:** 243–257, doi:10.1016/j.csr.2004.09.007

Plueddemann, A. J., and R. Pinkel. 1989. Characterization of the pattern of diel migration using Doppler sonar. Deep-Sea Res. **36:** 509–530, doi:10.1016/0198-0149(89)90003-4

Ressler, P. H. 2002. Acoustic backscatter measurements with a 153 kHz ADCP in the northeastern Gulf of Mexico: Determination of dominant zooplankton and micronekton scatterers. Deep-Sea Res. I **49:** 2035–2051, doi:10.1016/S0967-0637(02)00117-6

Reynold, G. T., and R. A. Lutz. 2001. Sources of light in the deep ocean. Rev. Geophys. **39:** 123–136, doi:10.1029/1999RG000071

Riccobenne, G., and others. 2007. Deep seawater inherent optical properties in the Southern Ionian Sea. Astropart. Phys. **27:** 1–9, doi:10.1016/j.astropartphys.2006.08.006

Ringelberg, J. 2010. Diel vertical migration of zooplankton in lakes and oceans: Causal explanations and adaptive significances. Springer-Science, doi:10.1007/978-90-481-3093-1

Roe, H. S. J., G. Griffiths, M. Hartman, and N. Crisp. 1996. Variability in biological distributions and hydrography from concurrent Acoustic Doppler Current Profiler and SeaSoar surveys. ICES J. Mar. Sci. **53:** 131–138, doi:10.1006/jmsc.1996.0013

Smith, R. C., and K. Baker. 1981. Optical properties of the clearest natural waters. Appl. Opt. **2:** 177–184, doi:10.1364/AO.20.000177

Steinberg, D. K., C. A. Carlson, N. R. Bates, S. A. Goldthwait, L. P. Madin, and A. F. Michaels. 2000. Zooplankton vertical migration and the active transport of dissolved organic and inorganics carbon in the Sargasso Sea. Deep-Sea Res. I **47:** 137–158, doi:10.1016/S0967-0637(99)00052-7

Tarling, G. A., F. Buchholz, and J. B. L. Matthews. 1999. The effect of a lunar eclipse on the vertical migration behaviour of *Meganyctiphanes norvegica* (Crustacea: Euphausiacea) in the Ligurian Sea. J. Plankton Res. **21:** 1475–1488, doi:10.1093/plankt/21.8.1475

van Haren, H. 2007. Monthly periodicity in acoustic reflections and vertical motions in the deep ocean. Geophys. Res. Lett. **34:** L12603, doi:10.1029/2007GL029947

Vinogradov, M. E. 1962. Feeding of the deep-sea zooplankton. Rapp. P.-V. Reun. - Cons. Int. Explor. Mer **153:** 114–119.

Wiebe, P. H., N. J. Copley, and S. H. Boyd. 1992. Coarse-scale horizontal patchiness and vertical migration of zooplankton in Gulf-Stream warm-core ring 82-H. Deep-Sea Res. **39:** S247–S278, doi:10.1016/S0198-0149(11)80015-4

Wilson, S. E., D. K. Steinberg, and K. O. Buesseler. 2008. Changes in fecal pellet characteristics with depth as indicators of zooplankton repackaging of particles in the mesopelagic zone of the subtropical and subarctic North Pacific Ocean. Deep-Sea Res. II **55:** 1636–1647, doi:10.1016/j.dsr2.2008.04.019

Yamaguchi, A., and others. 2002. Structure and size distribution of plankton communities down to the greater depths in the western North Pacific Ocean. Deep-Sea Res. II **49:** 5512–5529, doi:10.1016/S0967-0645(02)00205-9

Young, R. E. 1983. Oceanic bioluminescence: An overview of general functions. Bull. Mar. Sci. **33:** 829–845.

———, E. M. Kampa, S. D. Maynard, F. M. Mencher, and C. F. E. Roper. 1980. Counter illumination and the upper depth limits of midwater animals. Deep-Sea Res. **27:** 671–691, doi:10.1016/0198-0149(80)90022-9

Zhang, X., and H. G. Dam. 1997. Downward export of carbon by diel migrant mesozooplankton in the central equatorial Pacific. Deep-Sea Res. II **44:** 2191–2202, doi:10.1016/S0967-0645(97)00060-X

Associate editor: Thomas Kiørboe

Received: 13 August 2012
Accepted: 17 December 2012
Amended: 11 February 2013

19395590, 2013, 4, Downloaded from https://aslopubs.onlinelibrary.wiley.com/doi/10.4319/lo.2013.58.4.1207 by Moss Landing Marine Labs, Wiley Online Library on [06/11/2026]. See the Terms and Conditions (https://onlinelibrary.wiley.com/terms-and-conditions) on Wiley Online Library for rules of use; OA articles are governed by the applicable Creative Commons License